Computers & Graphics (2020)

Contents lists available at ScienceDirect

Computers & Graphics

journal homepage: www.elsevier.com/locate/cag

Curve guided T-spline skinning for surface and solid generation

Chuanfeng Hu[a], Jiaming Ai[a], Hongwei Lin[a,b,*]

[a] School of Mathematics, Zhejiang University, Hangzhou, Zhejiang province, China
[b] State Key Lab. of CAD&CG, Zhejiang University, Hangzhou, Zhejiang province, China

ARTICLE INFO

Article history:

2008 MSC: 68U05, 97R60

Keywords: T-spline, Surface skinning, Solid modeling, Iso-geometric analysis

ABSTRACT

Skinning is an essential technology in geometric modeling. Unlike non-uniform rational B-spline (NURBS) skinning, T-spline skinning does not require knot compatibility of the given cross-sections, and avoids superfluous of control points. In this study, we present a curve guided T-spline (CGTS) skinning method for surface and solid generation of high quality, which interpolates the given cross-sections. *Guiding curves* and least squares progressive and iterative approximation (LSPIA) method are involved in the CGTS skinning. Specifically, the guiding curves provide a visually pleasing shape for the skinned surface and solid, and the LSPIA method simplifies the iterative procedure, ensures the fitting accuracy, and shape preservation. On one hand, the CGTS surface skinning generates a visually pleasing and fairing skinned T-spline surface, which avoids the wiggle and crease problems. On the other hand, the CGTS solid skinning with optimization generates a trivariate T-spline solid with high quality. To meet the requirement of iso-geometric analysis (IGA) for the skinned T-spline solid, an optimization approach is employed in the solid skinning to improve the quality of the skinned T-spline solid. Finally, the experimental examples presented in this paper demonstrate the effectiveness and efficiency of the CGTS skinning method.

1. Introduction

Surface skinning, also known as lofting, is a process of constructing a surface from a set of cross-sections [1], which has been widely used in shipbuilding, automobile, and aviation industry [2]. The lofting can be traced back to the period of manual design. In the early works of hull design, designers usually took sample points on each cross-section of the hull, and subsequently, either interpolated or approximated the sample points by non-uniform rational B-spline (NURBS) curves, called cross-sections. Therefore, a surface is constructed by skinning the cross-sections.

As NURBS surface is becoming an industry standard for representing freeform shapes, it is a common process to generate skinned NURBS surfaces [3] from a set of cross-sections. Usually, the cross-sections represented by NURBS have different degrees and independent knot vectors. To solve the incompatibility, degree elevation and knot insertion are employed [4], resulting in the explosion of knots and control points.

Sederberg et al. [5] presented T-spline as a generalization of NURBS, giving more flexibility in representing complex surface shapes with fewer control points than NURBS surfaces. Therefore, some T-spline surface skinning methods are developed to overcome the knot compatibility problem. However, wiggles will appear on the skinned surface if common knots between the adjacent curves are too few [6], and creases are unavoidably generated by the improved T-spline surface skinning method [7].

In this study, a curve guided T-spline (CGTS) skinning method for surface and solid generation of high quality is presented, thus overcoming the knot compatibility problem and in-

*Corresponding author.
e-mail: hwlin@zju.edu.cn (Hongwei Lin)

terpolating all the given cross-sections. The CGTS surface skinning method is implemented by the following operations. First, an initial T-mesh is constructed by inserting intermediate cross-sections to the given cross-sections. In order to determine the best positions for the control points of the intermediate cross-sections, guiding curves are introduced to provide a fair shape of the given cross-sections along the longitudinal direction. Subsequently, some data points are sampled uniformly on the guiding curves, which are fitted with the skinned T-spline surface by several rounds of least squares progressive and iterative approximation (LSPIA) [8, 9]. Meanwhile, the control points of the T-spline surface are updated after each rounds of LSPIA, according to the *interpolated conditions*, which guarantees that the skinned surface interpolates the given cross-sections. Finally, a visually pleasing and fairing skinned T-spline surface is generated, avoiding the wiggle and crease problems. The CGTS solid skinning method is implemented similarly by interpolating the given cross-sectional T-spline surfaces. Furthermore, we adopt an optimization approach to improve the quality of the skinned T-spline solid. To summarize, the main contributions of this study are as follows:

- Guiding curves are applied for providing a visually pleasing shape for the skinned surface and solid.
- LSPIA method ensures the fitting accuracy and the stability of iterations.
- CGTS skinning method interpolating the given cross-sections for high quality surface and solid generation is proposed.

The remainder of this paper is organized as follows. In Section 1.1, we review related work on the surface skinning, solid modeling and iterative fitting. In Section 2, preliminaries on T-splines and T-spline surface skinning are introduced. The CGTS surface skinning method with high fairness is presented in Section 3. The CGTS solid skinning method with optimization is described in Section 4. In Section 5, some experimental examples are illustrated to demonstrate the effectiveness and efficiency of the CGTS skinning method. Finally, Section 6 concludes the paper.

1.1. Related work

Surface skinning: In general, surface skinning methods are mainly classified into two categories, namely approximation methods [4, 10, 11, 12] and interpolation methods [1, 3, 6, 7, 13]. The approximation methods can approximate the skinned surface within given error bounds. The given curves can be rebuilt within the error bounds, and the explosion of the control points can be removed. The interpolation methods usually are applied when generating an interpolatory skinned surface.

As a generalization of NURBS surfaces, a T-spline surface permits T-junctions in its T-mesh, which enables local refinement[5]. Numerous T-spline surface skinning methods were proposed to overcome the knot compatibility problem [12, 6, 14, 7]. Yang and Zheng [12] presented an approximate T-spline skinning method, which fitting the input rows of data points within a prescribed tolerance. An interpolation T-spline skinning method was developed by Nasri et al. [6] by inserting an intermediate cross-section between the given cross-sections. However, the wiggle problem will appear if common knots between the adjacent curves are too few. The surface skinning method was extended to periodic T-spline in semi-NURBS form by Li et al. [14], who addressed the wiggle problem and reduced the wiggle effect using 4-point interpolatory subdivision scheme [15] to derive the intermediate cross-sections. Oh et al. [7] provided a fundamental solution to avoid wiggles by adding two intermediate cross-sections, while major crease problem occurs on the skinned surface. Engleitner and Jüttler [13] applied the framework of patchwork B-splines to the construction of interpolated skinned surfaces, which not only reduces the resulting data volume but also limits the propagation of derivative discontinuities.

Solid modeling: NURBS and T-spline solid modeling methods are developed mainly for producing the three-dimensional physical domain in iso-geometric analysis (IGA) [16]. Specifically, Zhang et al. [17] introduced a skeleton-based method of generating NURBS solids through analyzing arterial blood flow in IGA. A cylinder-like trivariate B-spline solid was generated through harmonic-function-based volumetric parameterization [18]. Aigner et al. [19] presented a variational framework for generating NURBS solid by parameterizing a swept volume based on the given boundary conditions and guiding curves. Optimization approaches have been developed for filling boundary-represented models to produce trivariate B-spline solids with positive Jacobian value [20, 21]. Moreover, Lin et al. [22] presented a discrete volume parameterization method for tetrahedral mesh models and an iterative fitting algorithm for trivariate B-spline solids generation. The method was improved [23, 24] by applying pillow operation and geometric optimization to guarantee the generated B-spline solids with positive Jacobian value.

Due to the flexibility of T-splines in representing complex shapes with fewer control points than NURBS, T-spline solid modeling methods have been intensively studied. Escobar et al. [25] constructed T-spline solids using fitting triangular mesh models with zero-genus. Moreover, a mapping-based rational T-spline solid construction method was presented for zero-genus topology as well [26]. Wang et al. [27] proposed a method of constructing T-spline solids using boundary triangulations with an arbitrary genus topology by polycube mapping.

Iterative fitting: The progressive-iterative approximation (PIA) was first proposed in Refs. [28, 29], which is an iterative fitting method with explicit geometric meanings, advancing the handling of the geometric problems in the field of geometric design. In Ref. [30], the PIA method was proved to be convergent for NURBS. A local format of the PIA method was developed in [31]. Subsequently, the PIA format was extended to subdivision surface fitting [32]. To avoid the limitation of the PIA method that the number of the control points must be equal to that of the data points, some extended iterative fitting formats were developed to approximate the given data points, namely, extended PIA (EPIA) [33] and LSPIA [8, 9].

2. Preliminaries

Preliminaries on T-spline, LSPIA with T-splines and T-spline surface skinning are introduced in this section.

2.1. T-splines

For a T-spline surface, each control point $P_i, i = 0, 1, \cdots, m$, corresponds to a basis function:

$$B_i(u,v) = \frac{\omega_i R_i(u,v)}{\sum_{j=0}^{m} \omega_j R_j(u,v)},\ i = 0, 1, \cdots, m. \tag{1}$$

In Eq.(1), ω_i are nonnegative weights, which are set to 1 in the study according to the previous work [6, 7], and $R_i(u,v)$ are the blending functions,

$$R_i(u,v) = N[u_{i0}, u_{i1}, u_{i2}, u_{i3}, u_{i4}](u) M[v_{i0}, v_{i1}, v_{i2}, v_{i3}, v_{i4}](v), \tag{2}$$

where $N[u_{i0}, u_{i1}, u_{i2}, u_{i3}, u_{i4}](u)$ and $M[v_{i0}, v_{i1}, v_{i2}, v_{i3}, v_{i4}](v)$ are cubic B-spline basis function defined on the u-directional and v-directional knot vectors, respectively,

$$\boldsymbol{u}_i = [u_{i0}, u_{i1}, u_{i2}, u_{i3}, u_{i4}],\ \boldsymbol{v}_i = [v_{i0}, v_{i1}, v_{i2}, v_{i3}, v_{i4}]. \tag{3}$$

The local knot vectors $\boldsymbol{u}_i$ and $\boldsymbol{v}_i$ (Eq.(3)) can be determined by surrounding knots with the ray-method in the T-mesh [34]. Therefore, after obtaining the basis functions $B_i(u,v)$, $i = 0, 1, \cdots, m$, corresponding to the control points P_i, the T-spline surface $S(u,v)$ can be generated.

$$S(u,v) = \sum_{i=0}^{m} P_i B_i(u,v),\ i = 0, 1, \cdots, m. \tag{4}$$

Additionally, a T-spline solid can be represented by

$$V(u,v,w) = \sum_{i=0}^{m} P_i B_i(u,v,w),\ i = 0, 1, \cdots, m, \tag{5}$$

where $B_i(u,v,w)$ are the basis functions, which can be defined similarly using the above formulas.

2.2. LSPIA with T-splines

The LSPIA is performed for fitting a given set of data points by a T-spline surface or solid. In each iterative step, *difference vectors* related to the data points are calculated, and then *adjusting vector* for each control point is calculated, which is a weighted sum of the difference vectors. At last, the new T-spline surface or solid is obtained by adding the adjusting vectors to the control points. The iterations are terminated when either the fitting accuracy meets a preset accuracy or the number of iterations exceeds a preset iteration time.

Take a T-spline surface fitting by the LSPIA as an example. We start with an initial T-spline surface and suppose that the iteration has been performed for k steps, and the k-th T-spline surface $S^{(k)}(u,v)$ is generated,

$$S^{(k)}(u,v) = \sum_{i=0}^{m} P_i^{(k)} B_i(u,v).$$

One iteration step for producing $S^{(k+1)}(u,v)$ from $S^{(k)}(u,v)$ includes the following operations.

First, the *difference vector* for each data point is calculated,

$$\delta_l^{(k)} = Q_l - S^{(k)}(u_l, v_l),$$

where $Q_l,\ l = 0, 1, \cdots, L$ with parameters (u_l, v_l) are the data points. Each vector $\delta_l^{(k)}$ is distributed to the control points $P_i^{(k)}$, forming the *adjusting vector* for each control point,

$$\Delta_i^{(k)} = \frac{\sum_{l \in L_i} B_i(u_l, v_l) \delta_l^{(k)}}{\sum_{l \in L_i} B_i(u_l, v_l)},$$

where L_i is the index set of l such that $B_i(u_l, v_l) \neq 0$. Next, the control point $P_i^{(k+1)}$ for the $(k+1)$-th surface is obtained by adding the vector $\Delta_i^{(k)}$ to the control point $P_i^{(k)}$,

$$P_i^{(k+1)} = P_i^{(k)} + \Delta_i^{(k)}.$$

Thus, the $(k+1)$-th T-spline surface is generated.

These iterations are terminated when either the fitting accuracy meets a preset accuracy or the number of iterations exceeds a preset iteration time. The convergence of the LSPIA method has been proven in [8]

2.3. T-spline surface skinning

The T-spline surface skinning method interpolating the given cross-sections was first proposed by Nasri et al. [6], abbreviated as *Nasri's skinning method*. Subsequently, Oh et al. [7] enhanced the skinning method to avoid wiggle problem by adding one more intermediate cross-section between the given cross-sections, abbreviated as *Oh's skinning method*. The two algorithms are implemented by the construction of T-mesh and calculation of control points.

Construction of T-mesh: Given a set of ordered cross-sections represented by B-splines with independent knot vectors. The given curves are represented as:

$$C^i(u) = \sum_{j \in I_i} V_j^i N_j^i(u),\ i = 0, \cdots, n, \tag{6}$$

where $I_i,\ i = 0, \cdots, n$ are the index sets of the control points of the given curves, V_j^i are the control points and N_j^i are the corresponding B-spline basis functions. The parameters of the given curves in v-direction can be determined by the chord length parameterization [3]. Moreover, to interpolate the given cross-sections, one or two intermediate cross-sections are added between the given cross-sections. For the case that adding one intermediate cross-section, the knots of the added cross-sections are the common knots of two adjacent given cross-sections (Fig. 1(a)). For the other case, the knots of the added cross-sections are consistent with the knots of the nearest given cross-section (Fig. 1(b)). Following this, a control mesh is constructed for the given cross-sections and the added intermediate cross-sections. Therefore, if two adjacent cross-sections have a common knot, the longitudinal edge is connected. After all longitudinal edges are connected, the initial T-mesh is constructed completely, as shown in Fig. 1. In this study, the initial T-mesh of the CGTS skinning method is constructed in the same way.

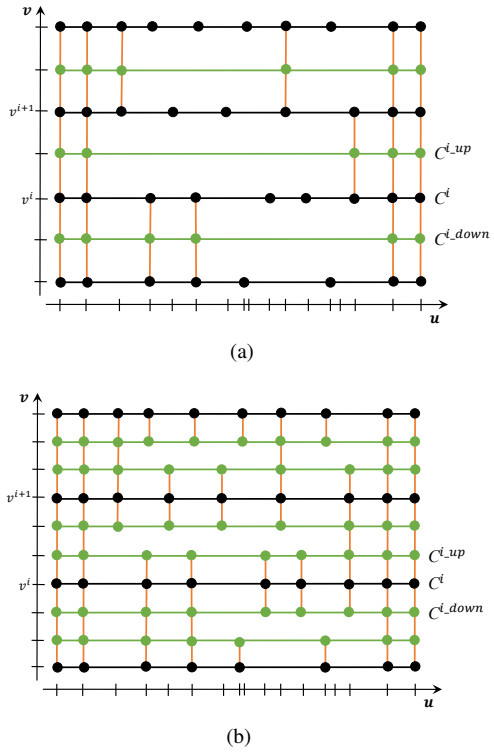

Fig. 1. Cross-sections to be skinned for pre-image of T-mesh, where the black lines are the given cross-sections to be interpolated, the green lines are the added intermediate cross-sections, and the orange lines are the longitudinal edges. (a) One intermediate cross-section between the given cross-sections. (b) Two intermediate cross-sections between the given cross-sections.

Calculation of control points: Suppose that $S(u, v)$ is the skinned T-spline surface. The control points in the T-mesh are calculated for interpolating the given cross-sections by the following *interpolation conditions*,

$$C^i(u) = S(u, v^i),\ i = 0, 1, \cdots, n, \tag{7}$$

where v^i is the v-directional parameter of the i-th given curve. As the interpolation of the curve is affected by two adjacent curves, Eq. (7) can be rewritten as:

$$\sum_{j\in I_i} V_j^i N_j^i(u) = \sum_{j\in I_{i\_up}} W_j^{i\_up} N_j^{i\_up}(u) M_j^{i\_up}(v^i) + \sum_{j\in I_i} W_j^i N_j^i(u) M_j^i(v^i) + \sum_{j\in I_{i\_down}} W_j^{i\_down} N_j^{i\_down}(u) M_j^{i\_down}(v^i), \tag{8}$$

where $W_j^{i\_up}$, W_j^i, and $W_j^{i\_down}$ are the control points of C^{i_up}, C^i, and C^{i_down}, respectively, which composite the control points of the T-spline surface. It is noteworthy that the two first and last given curves are interpolated with multiple knots. For the control points of C^{i_up}, C^i, or C^{i_down}, the v-directional knot vectors are the same. Therefore, $M_j^{i\_up}(v^i)$, $M_j^i(v^i)$, and $M_j^{i\_down}(v^i)$ can be replaced by three constants, a^i, b^i, and c^i, respectively.

For adding one intermediate cross-section between the given cross-sections, knot intersection to the curves C^{i_up} and C^{i_down} can ensure that the basis functions $N_j^{i\_up}(u)$ and $N_j^{i\_down}(u)$ coincide with $N_j^i(u)$. Therefore, we can obtain a system of equations,

$$V_j^i = a^i \widetilde{W}_j^{i\_up} + b^i W_j^i + c^i \widetilde{W}_j^{i\_down},\ j \in I_i,\ i = 1, \cdots, n-1, \tag{9}$$

where $\widetilde{W}_j^{i\_up}$ and $\widetilde{W}_j^{i\_down}$ are control points calculated from knot insertion to the added intermediate cross-sections C^{i_up} and C^{i_down}, respectively.

For adding two intermediate cross-sections between the given cross-sections, the u-directional knot vectors of C^{i_up} and C^{i_down} are the same as C^i and the basis functions $N_j^{i\_up}(u)$ and $N_j^{i\_down}(u)$ coincide with $N_j^i(u)$. Thus, we have,

$$V_j^i = a^i W_j^{i\_up} + b^i W_j^i + c^i W_j^{i\_down},\ j \in I_i,\ i = 1, \cdots, n-1. \tag{10}$$

Consequently, replacing V_j^i by W_j^i, the skinned T-spline surface that interpolates the given cross-sections is generated. However, in case of Nasri's skinning method, which adds one intermediate cross-section between the given cross-sections, wiggles will appear on the skinned T-spline surface if the given cross-sections are not sufficiently compatible, as shown in Fig. 2(e). In order to reduce the wiggles in the skinned surface, Oh's skinning method, which adds two intermediate cross-sections, was proposed. However, the intermediate cross-sections are added by linear interpolation, causing major crease problems on the skinned surface, as shown in Fig. 2(f).

3. CGTS surface skinning with high fairness

Unlike the approximate T-spline skinning method proposed by Yang and Zheng [12], the given cross-sections can be interpolated by the proposed CGTS skinning method in this study. The whole algorithm for the CGTS surface skinning method is illustrated in Algorithm 1. Specifically, given a set of ordered cross-sections as input, a series of iso-parametric points are sampled on the given cross-sections. By linearly interpolating the iso-parametric points along the longitudinal direction, some *linear interpolated points* on the intermediate cross-sections are generated. The intermediate cross-sections are initialized by fitting the interpolated points. Meanwhile, the iso-parametric points are also used to produce several guiding curves, which can not only result in avoiding the wiggles and creases, but also provide a visually pleasing shape of the skinned surface. As illustrated in Fig. 3, the intermediate cross-sections and guiding curves are constructed. Then we sample some points on the guiding curves as data points to fit with the skinned T-spline surface. The LSPIA method is invoked in the data fitting, and the control points W_j^i are updated by the interpolation equations (9) or (10), after LSPIA. Therefore, a visually pleasing skinned T-spline surface without wiggles and creases is generated.

In this study, two approaches to implement the CGTS surface skinning method are provided, including adding one or two intermediate cross-sections between the given cross-sections, abbreviated as *CGTS with one mid-section* and *CGTS with two mid-sections*. The details of the CGTS surface skinning method are elucidated in the following sections.

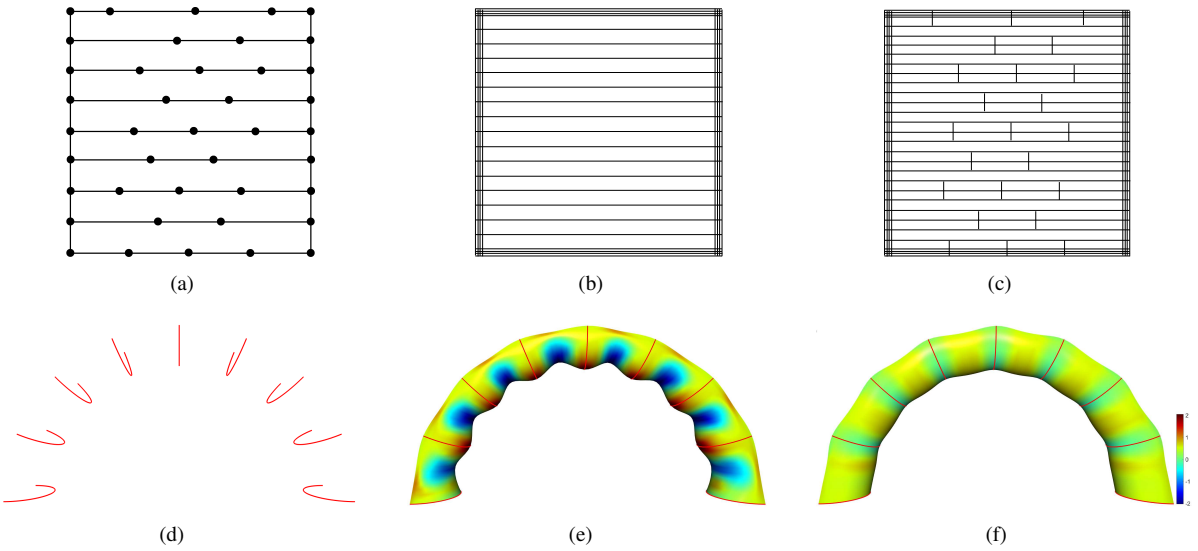

Fig. 2. Wiggles and creases appear on the skinned T-spline surfaces (*Torus*), where the color represents the distribution of the mean curvature. (a) Pre-image of the interpolated control mesh. (b) Pre-image of the T-mesh generated using Nasri's skinning method. (c) Pre-image of the T-mesh generated using Oh's skinning method. (d) The given cross-sections. (e) The skinned T-spline surface with wiggles generated using Nasri's skinning method. (f) The skinned T-spline surface with creases generated using Oh's skinning method.

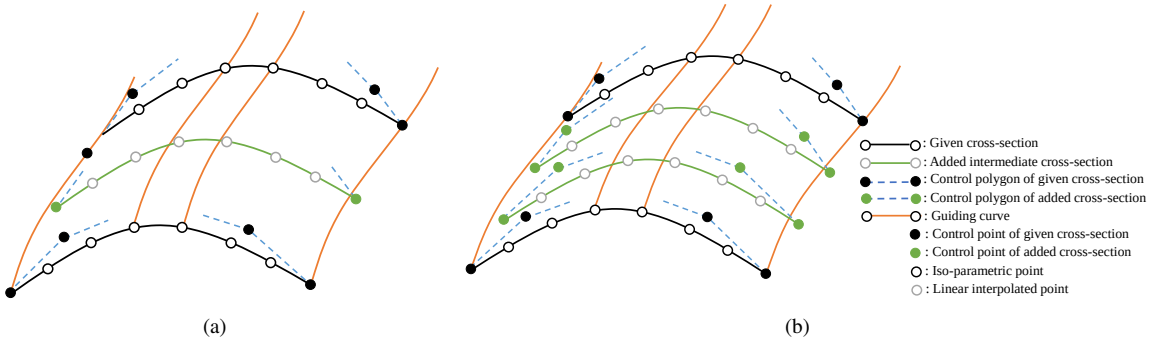

Fig. 3. Construction of the intermediate cross-sections and guiding curves from the iso-parametric points. (a) One added intermediate cross-section. (b) Two added intermediate cross-sections.

3.1. Guiding curve

The guiding curve is an important factor affecting the shape of the skinned surface. In order to ensure that the skinned T-spline surface is generated with high fairness, we sample a series of iso-parametric points on the given cross-sections to produce several interpolating B-spline curves, called *guiding curves*.

Suppose that $Q^i,\ i = 0, 1, \cdots, n$ are a set of ordered iso-parametric points along the longitudinal direction, a cubic B-spline curve interpolating the data points can be uniquely determined if the knots and two boundary conditions are given in advance [35]. An interpolating B-spline curve can be represented by the following formula,

$$C(v) = \sum_{i=0}^{n+2} P_i N_{i,3}(v), \tag{11}$$

with knot vector $\mathbf{v} = \{v^0, v^0, v^0, v^0, v^1, \cdots, v^{n-1}, v^n, v^n, v^n, v^n\}$ obtained from the T-mesh. In our implementation, the boundary conditions are taken as that, the second-order derivatives of the interpolating curve at two ends are both zero, i.e., $P''(v^0) = 0$ and $P''(v^n) = 0$. Then, the control points P_i of the interpolating B-spline curve can be calculated by the following equations,

$$\begin{aligned} Q^j &= C(v^j) = \sum_{i=0}^{n+2} P_i N_{i,3}(v^j),\ j = 0, 1, \cdots, n, \\ P_0 &= \frac{v^2 + v^1 - 2v^0}{v^2 - v^1} P_1 - \frac{v^1 - v^0}{v^2 - v^0} P_2, \\ P_{n+2} &= \frac{v^{n-1} - v^n}{v^n - v^{n-2}} P_n + \frac{2v^n - v^{n-1} - v^{n-2}}{v^n - v^{n-2}} P_{n+1}. \end{aligned} \tag{12}$$

By solving these linear equations, the interpolating B-spline curve can be generated. Therefore, a set of guiding curves represented by the interpolating B-splines can be constructed.

Algorithm 1 CGTS surface skinning method

Input: A set of cross-sections represented by B-splines and a predefined fitting iteration time τ and precision ε_0.

Output: A fairing skinned T-spline surface without wiggles and creases.

1. Sample iso-parametric points on the given cross-sections;
2. Insert the intermediate cross-sections;
3. Construct the initial T-mesh and the initial skinned T-spline surface;
4. Produce the guiding curves by interpolating the iso-parametric points;
5. Sample data points uniformly on the guiding curves;
6. $\alpha \leftarrow 0,\ \beta \leftarrow 0,\ \varepsilon \leftarrow 1$;
7. **while** $\varepsilon > \varepsilon_0$ and $\alpha \le \tau$ **do** //α-th round of LSPIA
8. **while** $\varepsilon > \varepsilon_0$ and $\beta \le \tau$ **do** //β-th step of iteration in the α-th round of LSPIA
9. Data fitting by the LSPIA method;
10. $\beta \leftarrow \beta + 1$;
11. **end while**
12. Update the control points for interpolating the given curves;
13. $\alpha \leftarrow \alpha + 1, \beta \leftarrow 0$;
14. **end while**

3.2. *Iterative fitting algorithm*

The guiding curves provide a visually pleasing shape for the skinned T-spline surface. As a result, only by fitting with the guiding curves can the skinned T-spline surface achieve high fairness. We employ the LSPIA method to fit the skinned T-spline surface with the guiding curves, by fitting with the data points sampled on the guiding curves. Meanwhile, the skinned T-spline surface needs to interpolate the given cross-sections. In this study, the iterative fitting is implemented by several rounds of LSPIA, and after each rounds of LSPIA the control points are updated for interpolation.

Denote that the T-spline surface generated by the β-th step of iteration in the α-th round of LSPIA is $S^{(\alpha,\beta)}(u,v)$. Assume that $Q_l,\ l = 0, 1, \cdots, L$ with parameters (u_l, v_l) are the data points sampled on the guiding curves. Start with an initial T-spline surface $S^{(0,0)}(u,v)$, which can be constructed from the initial T-mesh. Suppose that the iteration has been performed for β steps in α-th round of LSPIA, and the (α,β)-th skinned T-spline surface $S^{(\alpha,\beta)}(u,v)$ is generated,

$$S^{(\alpha,\beta)}(u,v) = \sum_{i=0}^{m} P_i^{(\alpha,\beta)} B_i(u,v). \tag{13}$$

And the $(\alpha,\beta+1)$-th skinned T-spline surface $S^{(\alpha,\beta+1)}(u,v)$ is produced by the following operations.

The *difference vector* for each data point is calculated,

$$\delta_l^{(\alpha,\beta)} = Q_l - S^{(\alpha,\beta)}(u_l, v_l). \tag{14}$$

Each difference vector $\delta_l^{(\alpha,\beta)}$ distributes the weighted vector $B_i(u_l,v_l)\delta_l^{(\alpha,\beta)}$ to the control point $P_i^{(\alpha,\beta)}$, whose corresponding basis function is not equal to zero. Consequently, the *adjusting vector* for each control point is generated,

$$\Delta_i^{(\alpha,\beta)} = \frac{\sum_{l\in L_i} B_i(u_l,v_l)\delta_l^{(\alpha,\beta)}}{\sum_{l\in L_i} B_i(u_l,v_l)}, \tag{15}$$

where L_i is the index set of l such that $B_i(u_l,v_l) \neq 0$. Therefore, the control points of the $(\alpha,\beta+1)$-th skinned T-spline surface can be formed,

$$P_i^{(\alpha,\beta+1)} = P_i^{(\alpha,\beta)} + \Delta_i^{(\alpha,\beta)}. \tag{16}$$

The iterations in the α-th round of LSPIA are terminated when either $\varepsilon = \left| \frac{\sum_l \left\|\delta_l^{(\alpha,\beta+1)}\right\|^2}{\sum_l \left\|\delta_l^{(\alpha,\beta)}\right\|^2} - 1 \right| < \varepsilon_0$ or the number of iterations exceeds a predefined fitting iteration time, τ. After each rounds of the LSPIA, the control points are updated by Eq. (9) or Eq. (10) for interpolating the given cross-sections. Now, the $(\alpha+1,0)$-th T-spline surface is obtained. Define the error of the α-th round of data fitting as $\sum_l \left\|\delta_l^{(\alpha)}\right\|^2 = \sum_l \left\|\delta_l^{(\alpha+1,0)}\right\|^2$. The whole iterative fitting procedure is terminated when either $\varepsilon = \left| \frac{\sum_l \left\|\delta_l^{(\alpha)}\right\|^2}{\sum_l \left\|\delta_l^{(\alpha-1)}\right\|^2} - 1 \right| < \varepsilon_0$ or the number of rounds exceeds τ. In our implementation, we take $\varepsilon_0 = 10^{-4}$ and $\tau = 20$.

The experimental results are showing that the iterative fitting method in this study has the approximate convergence as the LSPIA method. We have demonstrated the CGTS surface skinning method to skin the same curves (Fig. 2(d)), and the average fitting errors $\frac{\sum_l \left\|\delta_l^{(s,t)}\right\|^2}{L+1}$ with respect to iteration counts are shown in Fig. 4. After each rounds of LSPIA, the control points are updated for interpolation, and the curves of the iteration counts versus average fitting error will appear a peak. However, as the iteration goes on, the peak becomes smaller than before and the average fitting error converges gradually.

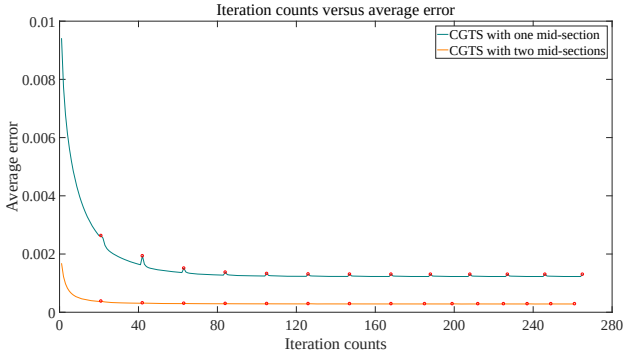

Fig. 4. Iteration counts versus average error. The red circles are the average errors after updating the control points for interpolation.

The skinned surfaces generated by the CGTS surface skinning method are shown in Fig. 5. Our developed surface skinning method obviously improves the quality of the skinned T-spline surface (Figs. 5(c) and 5(d)), which removes the wiggles(Fig. 2(e)) and creases(Fig. 2(f)). Fig. 5(a) presents the guiding curves constructed by the given cross-sections with C^2 continuity. Fig. 5(b) shows the data points sampled on the guiding curves, which keep the shape of the guiding curves. By

fitting to the data points, the skinned T-spline surfaces are generated. Therefore, the quality of the skinned T-spline surface in Fig. 5(c) is better than that of the T-spline surface in Fig. 2(f) with fewer control points. Additionally, the skinned T-spline surface in Fig. 5(d) is fairest than the other skinned surfaces. And statistical data are listed in Tables 1 and 2.

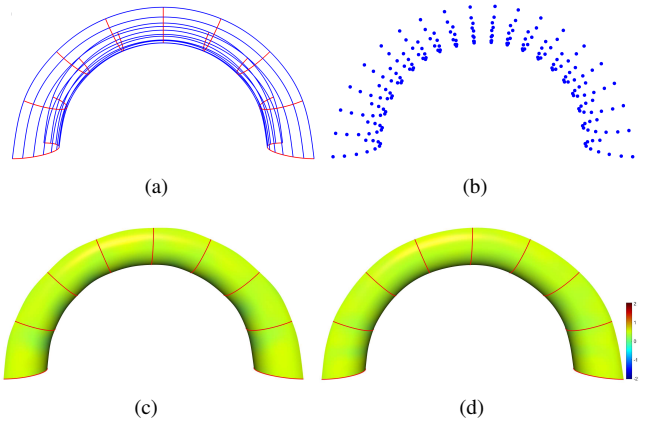

Fig. 5. Skinned surfaces generated by the CGTS skinning method with mean curvature distribution (*Torus*). (a) The given cross-sections (curves in red) and the guiding curves (curves in blue). (b) The data points sampled on the guiding curves. (c) CGTS with one mid-section. (d) CGTS with two mid-sections.

4. CGTS solid skinning with optimization

With the advent of iso-geometric analysis (IGA), which is a numerical analysis method based on spline theory, creating spline solids efficiently for IGA is becoming an urgent problem in the field of solid modeling. In this study, the CGTS solid skinning method is developed. Given a set of ordered cross-sectional surfaces, and skinning them with T-splines, a trivariate T-spline solid can be generated, which interpolates the given T-spline surfaces. Furthermore, due to the fact the Jacobian value of every point in the spline solid for simulation needs to be greater than zero in IGA. an optimization approach is employed to improve the quality of the skinned T-spline solid.

The whole algorithm for the CGTS solid skinning method is illustrated in Algorithm 2. Specifically, given a set of ordered cross-sectional T-spline surfaces, a series of iso-parametric points are sampled on the given cross-sections. Similar to the surface skinning, several intermediate cross-sections are generated and added into the given cross-sections. In this study, two intermediate cross-sections are added between the given cross-sections, so that the skinned T-spline solid can achieve high quality. Then, the initial T-mesh and initial T-spline solid are constructed. Meanwhile, by interpolating the iso-parametric points, the guiding curves running through all the cross-sections are produced. Then we sample some data points on the guiding curves, and optimize them in order to generate the skinned T-spline solid with high quality. More concretely, a stitched B-spline solid is constructed by fitting the data points, and the stitched B-spline solid is optimized. Finally, we resample the B-spline solid at the same parameters of the data points to obtain the optimized data points. Therefore, by fitting to the optimized data points and interpolating the given cross-sections, the T-spline solid with high quality is generated.

Algorithm 2 CGTS solid skinning method

Input: A set of cross-sections represented by T-splines and a predefined fitting iteration times τ and precision ε_0.
Output: A skinned T-spline solid with high quality.

1. Sample iso-parametric points on the given cross-sectional T-spline surfaces;
2. Insert two intermediate cross-sections between the given cross-sections;
3. Construct the initial T-mesh and the initial skinned T-spline solid;
4. Produce the guiding curves by interpolating the iso-parametric points;
5. Sample data points uniformly on the guiding curves for constructing a stitched B-spline solid;
6. Optimize the stitched B-spline solid and resample data points from the B-spline solid;
7. $\alpha \leftarrow 0$, $\beta \leftarrow 0$, $\varepsilon \leftarrow 1$;
8. **while** $\varepsilon > \varepsilon_0$ and $\alpha \leq \tau$ **do** //α-th round of LSPIA
9. **while** $\varepsilon > \varepsilon_0$ and $\beta \leq \tau$ **do** //β-th step of iteration in the α-th round of LSPIA
10. Data fitting by the LSPIA method;
11. $\beta \leftarrow \beta + 1$;
12. **end while**
13. Update the control points for interpolating the given surfaces;
14. $\alpha \leftarrow \alpha + 1, \beta \leftarrow 0$;
15. **end while**

4.1. Solid skinning with two intermediate surfaces

Suppose that $S^i(u,v)$, $i = 0, 1, \cdots, n$ are the given cross-sectional surfaces, $S^{i\_up}(u,v)$ and $S^{i\_down}(u,v)$ are two intermediate cross-sectional surfaces adjacent to $S^i(u,v)$. The skinned T-spline solid $V(u,v,w)$ can be generated from the CGTS solid skinning method, and the control points in the T-mesh can be calculated by the following interpolation conditions,

$$S^i(u,v) = V(u,v,w^i),\ i = 0, 1, \cdots, n, \tag{17}$$

where w^i is the parameter of the i-th surface in the w-direction, which can be calculated by the chord length parameterization. Similar to the surface skinning method which adds two intermediate cross-sections between the given cross-sections, we can also get a system equations,

$$V_j^i = a^i W_j^{i\_up} + b^i W_j^i + c^i W_j^{i\_down},\ j \in I_i,\ i = 1, \cdots, n-1, \tag{18}$$

where V_j^i, $j \in I_i$ are the control points in the T-mesh of the i-th given cross-sectional T-spline surface, and $W_j^{i\_up}$, W_j^i and $W_j^{i\_down}$ are the control points of the cross-sections, which composite the control points of the skinned T-spline solid. By replacing V_j^i with W_j^i, the given cross-sections are interpolated. Analogously, the two first and last given T-spline surfaces are interpolated with multiple knots.

4.2. Optimization

To achieve the purpose that the skinned T-spline solid is generated with high quality, the data points are optimized by the following operations. Several connected B-spline solids are constructed between the given cross-sectional surfaces by fitting to the data points. The adjacent B-spline solids are C^0 continuous along the common boundary surface. After optimizing each B-spline solid independently, a stitched B-spline solid with high quality is constructed. Therefore, it is needed to resample the data points on the stitched B-spline solid with the same parameters, which are fitted with the T-spline solid.

The details of the optimization for a B-spline solid are illustrated as follows. First, a B-spline solid is represented as,

$$\mathcal{H}(u,v,w)=\sum_{i}^{I}\sum_{j}^{J}\sum_{k}^{K}H_{i,j,k}N_{i,p}(u)N_{j,q}(v)N_{k,r}(w), \tag{19}$$

where $H_{ijk},\ i=0,1,\cdots,I,\ j=0,1,\cdots,J,k=0,1,\cdots,K$ are control points, and $N_{i,p}(u)$, $N_{j,q}(v)$ and $N_{k,r}(w)$ are the B-spline basis functions of degree p,q,r in the u,v,w-direction, respectively. In this study, tri-cubic tensor product B-spline is adopted.

Denote the *difference vectors* as

$$\boldsymbol{T}^{u}_{ijk}=\frac{H_{i+1,j,k}-H_{i,j,k}}{\left\|H_{i+1,j,k}-H_{i,j,k}\right\|},\boldsymbol{T}^{v}_{ijk}=\frac{H_{i,j+1,k}-H_{i,j,k}}{\left\|H_{i,j+1,k}-H_{i,j,k}\right\|},$$
$$\boldsymbol{T}^{w}_{ijk}=\frac{H_{i,j,k+1}-H_{i,j,k}}{\left\|H_{i,j,k+1}-H_{i,j,k}\right\|},$$

Therefore, the Jacobian value of the B-spline solid is,

$$J(u,v,w)=\boldsymbol{H}_u(u,v,w)\cdot(\boldsymbol{H}_v(u,v,w)\times\boldsymbol{H}_w(u,v,w))$$
$$=\sum_{\mathcal{I}_u}\sum_{\mathcal{I}_v}\sum_{\mathcal{I}_w}\alpha_{\mathcal{I}_u\mathcal{I}_v\mathcal{I}_w}\left[\boldsymbol{T}^{u}_{i_uj_uk_u}\cdot(\boldsymbol{T}^{v}_{i_vj_vk_v}\times\boldsymbol{T}^{w}_{i_wj_wk_w})\right]B_{\mathcal{I}_u}(u)B_{\mathcal{I}_v}(v)B_{\mathcal{I}_w}(w),$$

where $\mathcal{I}_u=(i_u,i_v,i_w),\mathcal{I}_v=(j_u,j_v,j_w),\mathcal{I}_w=(k_u,k_v,k_w)$ are index sets, $\alpha_{\mathcal{I}_u\mathcal{I}_v\mathcal{I}_w}>0$, and,

$$B_{\mathcal{I}_u}(u)=B^{p-1}_{i_u}(u)B^{p}_{i_v}(u)B^{p}_{i_w}(u),B_{\mathcal{I}_v}(v)=B^{q}_{j_u}(v)B^{q-1}_{j_v}(v)B^{q}_{j_w}(v),$$
$$B_{\mathcal{I}_w}(w)=B^{r}_{k_u}(w)B^{r}_{k_v}(w)B^{r-1}_{k_w}(w).$$

If $\boldsymbol{T}^{u}_{i_uj_uk_u}\cdot(\boldsymbol{T}^{v}_{i_vj_vk_v}\times\boldsymbol{T}^{w}_{i_wj_wk_w})>0$ is ensured, the Jacobian values of the B-spline solid are all positive [20].

Denote the *unit vectors* as,

$$\boldsymbol{T}^{u}=\frac{\sum_{i,j,k}\boldsymbol{T}^{u}_{ijk}}{\left\|\sum_{i,j,k}\boldsymbol{T}^{u}_{ijk}\right\|},\quad\boldsymbol{T}^{v}=\frac{\sum_{i,j,k}\boldsymbol{T}^{v}_{ijk}}{\left\|\sum_{i,j,k}\boldsymbol{T}^{v}_{ijk}\right\|},\quad\boldsymbol{T}^{w}=\frac{\sum_{i,j,k}\boldsymbol{T}^{w}_{ijk}}{\left\|\sum_{i,j,k}\boldsymbol{T}^{w}_{ijk}\right\|}.$$

In this study, the optimization is formulated as the minimization of several energy functions employed in Ref. [23].

$$min_{H_{i,j,k}}E=(1-\mu-\nu)E_{fit}+\mu(E_u+E_v+E_w)+\nu(E_{uv}+E_{uw}+E_{vw}), \tag{20}$$

where $\mu,\nu\in[0,1]$ are weights. The objective function is elucidated in detail as follows,

1. Fitting precision to the data points.

$$E_{fit}=\sum_{l=0}^{N_l}\left\|\mathcal{H}(u_l,v_l,w_l)-Q_l\right\|^2,$$

where $Q_l,\ l=0,1,\cdots,N_l$ are the data points sampled on the guiding curves.

2. Validity improvement for the B-spline solid.

- *Difference vectors* in the same parameter direction are as parallel to each other as possible.

$$E_u=\frac{1}{N_u}\sum_{i,j,k}(1-\boldsymbol{T}^{u}_{ijk}\cdot\boldsymbol{T}^{u}),E_v=\frac{1}{N_v}\sum_{i,j,k}(1-\boldsymbol{T}^{v}_{ijk}\cdot\boldsymbol{T}^{v}),$$
$$E_w=\frac{1}{N_w}\sum_{i,j,k}(1-\boldsymbol{T}^{w}_{ijk}\cdot\boldsymbol{T}^{w}),$$

where N_u,N_v,N_w are the number of the vectors $\boldsymbol{T}^{u}_{ijk},\boldsymbol{T}^{v}_{ijk},\boldsymbol{T}^{w}_{ijk}$, respectively.

- *Difference vectors* in different parameter directions are as perpendicular to each other as possible.

$$E_{uv}=(\boldsymbol{T}^{u}\cdot\boldsymbol{T}^{v})^2,\quad E_{uw}=(\boldsymbol{T}^{u}\cdot\boldsymbol{T}^{w})^2,\quad E_{vw}=(\boldsymbol{T}^{v}\cdot\boldsymbol{T}^{w})^2.$$

As shown in Fig. 6, given a set of ordered cross-sectional surfaces (Fig. 6(a)) as the input to the CGTS solid skinning algorithm, a trivariate T-spline solid (Fig. 6(b)) is generated, and the mesh generated from the knots is drawn on the solid. We can see the interpolation of the given surfaces from a transparent solid in Fig. 6(c). In the cut-away view (Fig. 6(d)) of the iso-parametric mesh, the interior of the T-spline solid can be seen clearly. The statistical data are listed in Table 3.

5. Implementation, results and discussions

The CGTS skinning method is implemented using the C++ programming language and tested on a PC with a 3.60 GHz i7-4790 CPU and 16 GB RAM. In this section, some examples are presented, and implementation details are discussed.

5.1. Surface skinning

The CGTS surface skinning method in this study is compared with two previous T-spline surface skinning methods, presented in Refs. [6, 7], both of which interpolate the given cross-sections. In this section, some skinned surface results are presented (Figs. 5 and 7-9) to demonstrate the effectiveness and efficiency of CGTS surface skinning method. Moreover, statistical data are listed in the Table 1, including the number of the given cross-sections, added intermediate cross-sections, guiding curves, data points, and control points.

Due to the incompatible knots of the adjacent given cross-sections, there are some wiggles on the T-spline surfaces (Figs. 2(e), 7(b), 8(b) and 9(b)) skinned by Nasri's skinning method. To remove the wiggles, Oh's skinning method adds one more intermediate cross-section between the given cross-sections. However, some creases inevitably appear on the skinned T-spline surfaces (Figs. 2(f), 7(c), 8(c) and 9(c)), which cause the unfairness of the skinned surface.

Moreover, Nasri's and Oh's skinning methods do not pay attention to the fairness of the skinned surface. And the CGTS surface skinning method preserves the shape controlled by the guiding curves with C^2 continuity. As a result, the shape controlled by the guiding curves is smoother than that of the other two methods, and the skinned T-spline surface achieve high fairness.

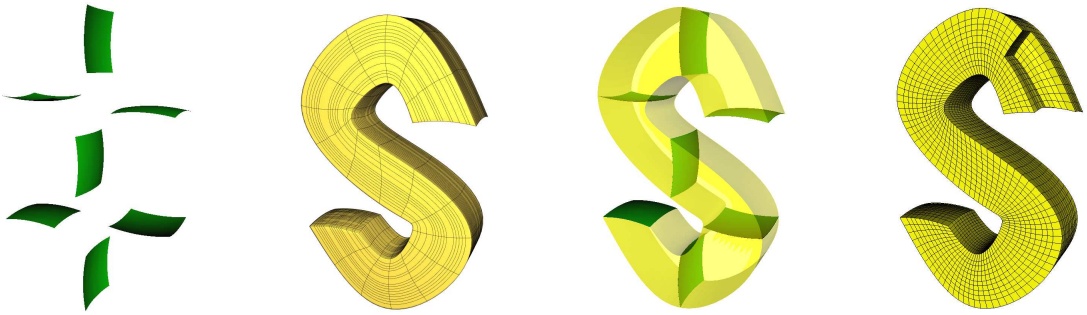

(a) (b) (c) (d)

Fig. 6. CGTS solid skinning (*S shape*). (a) The given cross-sectional T-spline surfaces. (b) The skinned T-spline solid with the mesh generated from the knots. (c) Transparent skinned solid with the given surfaces. (d) Cut-away view of the skinned solid.

By introducing the guiding curves and the LSPIA method into the skinning, the quality of the skinned surfaces (Figs. 5(c), 7(d), 8(d) and 9(d)) generated by the CGTS with one section is better than that by Oh's skinning method. In addition, the number of the control points of the surface generated by the CGTS with one section is less than using Oh's skinning method. Therefore, the skinned surfaces (Figs. 5(d), 7(e), 8(e) and 9(e)) generated by the CGTS with two mid-sections can not only remove the wiggles and creases, but also achieve high fairness. To show the quality of the skinned T-spline surfaces in detail, the results generated by the CGTS skinning method with two mid-sections are rendered with their own color scales, shown in Fig. 10.

As we can see from Table 2, the minimum and maximum mean curvature values of the skinned T-spline surface are presented. The ranges of the mean curvature values of the surfaces generated using Nasri's skinning method are largest than the others, meaning that wiggles appear on the skinned surfaces. And with Oh's skinning method and CGTS with one mid-section, the ranges of the mean curvature values are comparable. Significantly, the skinned surfaces generated by the CGTS with two mid-sections possess the largest minimum curvature value and the smallest maximum curvature value among the skinned surfaces, showing that the surfaces are generated with high quality. The largest minimum curvature value and smallest maximum curvature value in Table 2 are shown in bold.

5.2. Solid skinning

In this section, we describe the use of the CGTS solid skinning method to generate some trivariate T-spline solids (*Moai*, *Tooth* and *Duck*, shown in Figs. 11, 12 and 13, respectively). Table 3 lists the statistics in the solid skinning. The average scaled Jacobian value of the T-spline solid is defined as,

$$avg\_Jac = \frac{\int\int\int_{\Omega} Jac(x,y,z)dxdydz}{\int\int\int_{\Omega} dxdydz}, \qquad (21)$$

where $Jac(x,y,z)$ is the scaled Jacobian value [36] at (x,y,z).

It should be noted that the weights employed in the optimization to balance the energy functions are listed in Table 3. Moreover, for comparison, the minimum scaled Jacobian values, maximum scaled Jacobian values, and average scaled Jacobian values in the skinned T-spline solid before and after the optimization, are presented in Table 3. It can be seen that the minimum Jacobian values and average scaled Jacobian values in the skinned T-spline solids are improved after optimization. Although the Jacobian values can not be guaranteed to be all positive in theory, the minimum Jacobian values in our implementation are all positive. Therefore, the qualities of the T-spline solids are improved after the optimization.

6. Conclusion

In this study, we have presented a CGTS surface skinning method with high fairness to interpolate the given cross-sections. The wiggles and creases appearing in the skinning surfaces using Nasri's and Oh's skinning methods can be removed. The introduced guiding curves in the developed method provide a visually pleasing shape for the skinned surface. The LSPIA method not only simplifies the iterative process in Oh's skinning method, but also ensures the fitting accuracy and stability of iterations.

Furthermore, the CGTS skinning method is developed for the field of solid modeling to generate a skinned T-spline solid that interpolates the given cross-sectional T-spline surfaces. In order to make sure that the trivariate T-spline solid can be simulated in the framework of IGA, an optimization approach is employed in the skinning, which improves the quality of the skinned T-spline solid.

Acknowledgments

This paper is supported by the National Natural Science Foundation of China under Grant Nos. 61872316, 61932018.

References

[1] Woodward, CD. Skinning techniques for interactive B-spline surface interpolation. Computer-Aided Design 1988;20(8):441–451.
[2] Piegl, LA, Tiller, W. The NURBS Book. Berlin, Heidelberg: Springer Berlin Heidelberg; 1997.

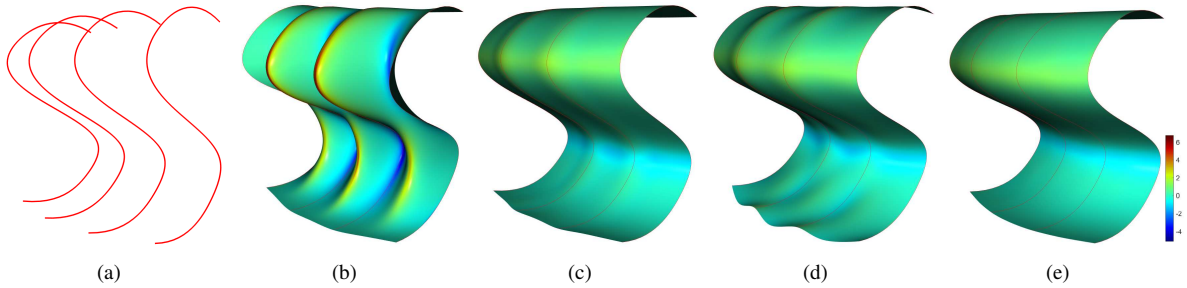

Fig. 7. Comparison of T-spline surface skinning methods with skinned surfaces with mean curvature distribution (*S shape*). (a) The given cross-sections. (b) Nasri's skinning method. (c) Oh's skinning method. (d) CGTS with one mid-section. (e) CGTS with two mid-sections.

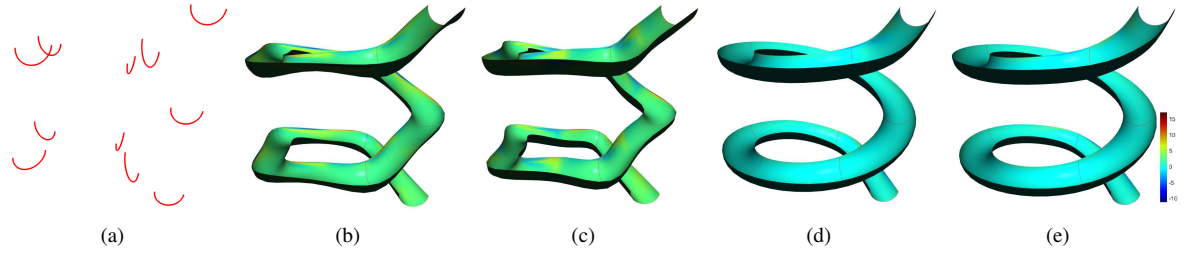

Fig. 8. Comparison of T-spline surface skinning methods with skinned surfaces with mean curvature distribution (*Helicoid*). (a) The given cross-sections. (b) Nasri's skinning method. (c) Oh's skinning method. (d) CGTS with one mid-section. (e) CGTS with two mid-sections.

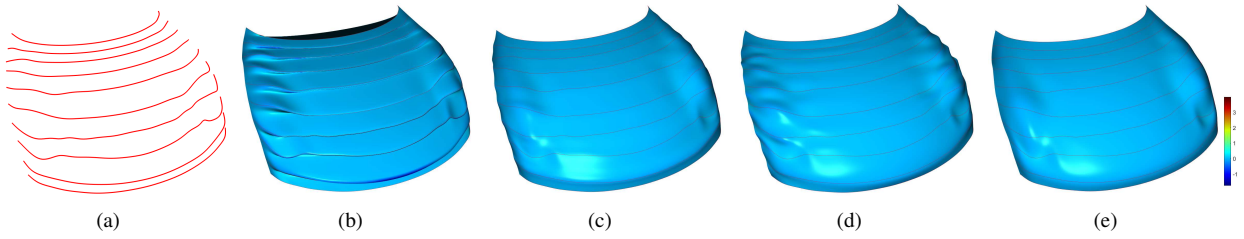

Fig. 9. Comparison of T-spline surface skinning methods with skinned surfaces with mean curvature distribution (*Bonnet*). (a) The given cross-sections. (b) Nasri's skinning method. (c) Oh's skinning method. (d) CGTS with one mid-section. (e) CGTS with two mid-sections.

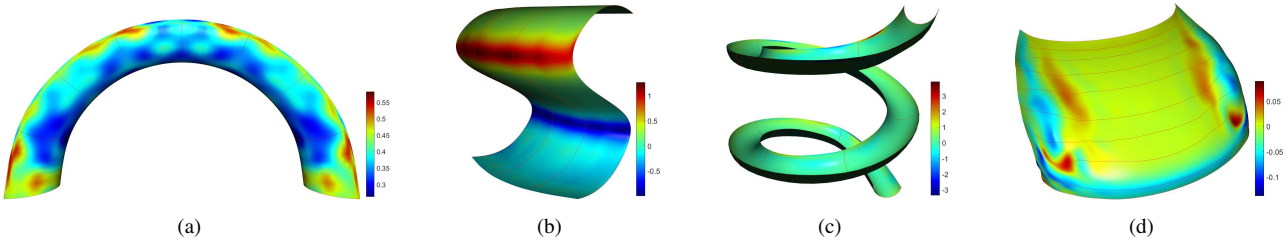

Fig. 10. T-spline surfaces skinned by the CGTS skinning method rendering with their own color scales. (a)*Torus*. (b)*S shape*. (c)*Helicoid*. (d)*Bonnet*.

[3] Piegl, LA, Tiller, W. Surface skinning revisited. Visual Computer 2002;18(4):273–283.
[4] Piegl, LA, Tiller, W. Algorithm for approximate NURBS skinning. Computer-Aided Design 1996;28(9):699–706.
[5] Sederberg, TW, Zheng, J, Bakenov, A, Nasri, A. T-splines and T-NURCCs. Transactions on Graphics 2003;22(3):477–484.
[6] Nasri, A, Sinno, K, Zheng, J. Local T-spline surface skinning. Visual Computer 2012;28(6-8):787–797.
[7] Oh, MJ, Roh, MI, Kim, TW. Local T-spline surface skinning with shape preservation. Computer-Aided Design 2018;104:15–26.
[8] Lin, H, Zhang, Z. An efficient method for fitting large data sets using T-splines. SIAM Journal on Scientific Computing 2013;35(6):A3052–

Table 1. Statistical data of T-spline surface skinning.

Model	*Torus/S shape/Helicoid/Bonnet*			
#Given curves[a]	9/4/11/10			
Method	#Added curves[b]	#Guiding curves[c]	#Data points[d]	#Control points[e]
Nasri's skinning method	8/3/10/9	-	-	105/66/121/283
Oh's skinning method	16/6/20/18	-	$16 \times 20/6 \times 20/20 \times 20/18 \times 40$	177/108/216/624
CGTS with one mid-section	8/3/10/9	10/10/15/20	$10 \times 20/10 \times 20/15 \times 20/20 \times 40$	105/66/121/283
CGTS with two mid-sections	16/6/20/18	10/10/15/20	$10 \times 20/10 \times 20/15 \times 20/20 \times 40$	177/108/216/624

[a] Number of the given cross-sections.
[b] Number of the added intermediate cross-sections.
[c] Number of the guiding curves.
[d] Number of the data points.
[e] Number of the the control points.

Table 2. Minimum and maximum mean curvature value of skinned surfaces.

Method	*Torus*		*S shape*		*Helicoid*		*Bonnet*	
	min_Cur.[a]	max_Cur.[b]	min_Cur.	max_Cur.	min_Cur.	max_Cur.	min_Cur.	max_Cur.
Nasri's skinning method	-2.0377	2.0526	-5.1588	6.7496	-11.2045	17.0009	-1.7564	3.9871
Oh's skinning method	-0.2920	0.7945	-1.1828	1.5509	-8.2984	17.2117	-0.1842	0.0634
CGTS with one mid-section	0.1880	0.5822	-2.5958	1.8404	-3.9537	5.1236	-0.2450	0.1248
CGTS with two mid-sections	**0.2624**	**0.5694**	**-0.9970**	**1.2605**	**-3.3599**	**3.9016**	**-0.1379**	**0.0899**

[a] Minimum mean curvature value.
[b] Maximum mean curvature value.

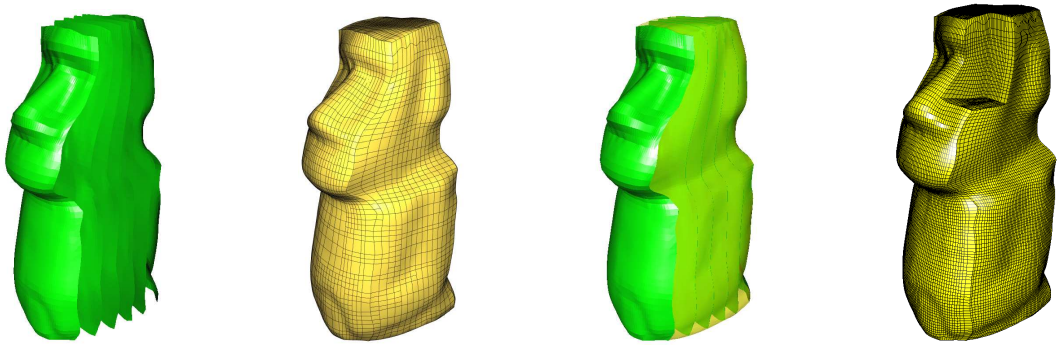

(a) (b) (c) (d)

Fig. 11. CGTS solid skinning (*Moai*). (a) The given cross-sectional T-spline surfaces. (b) The skinned T-spline solid with the mesh generated from the knots. (c) Transparent skinned solid with the given surfaces. (d) Cut-away view of the skinned solid.

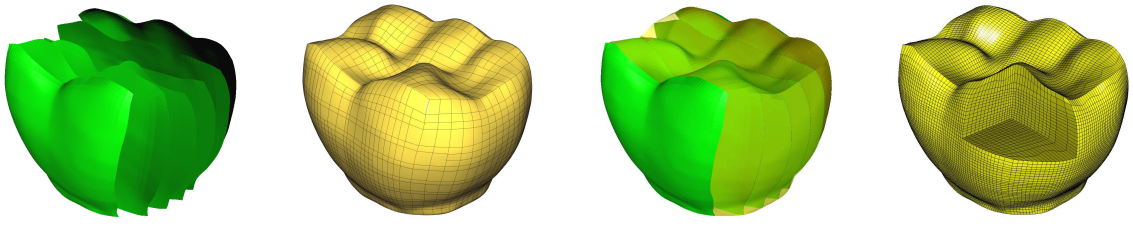

(a) (b) (c) (d)

Fig. 12. CGTS solid skinning (*Tooth*). (a) The given cross-sectional T-spline surfaces. (b) The skinned T-spline solid with the mesh generated from the knots. (c) Transparent skinned solid with the given surfaces. (d) Cut-away view of the skinned solid.

A3068.
[9] Deng, C, Lin, H. Progressive and iterative approximation for least squares B-spline curve and surface fitting. Computer-Aided Design 2014;47(1):32–44.
[10] Park, H, Kim, K, Lee, S. A method for approximate NURBS curve compatibility based on multiple curve refitting. Computer-Aided Design 2000;32(4):237–252.
[11] Park, H. An approximate lofting approach for B-spline surface fitting to functional surfaces. International Journal of Advanced Manufacturing Technology 2001;18(7):474–482.

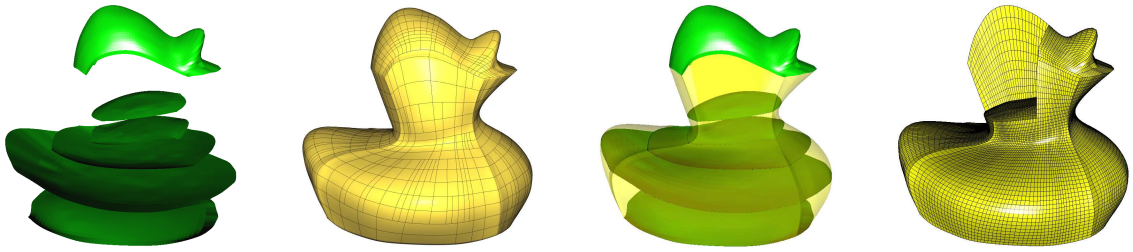

(a) (b) (c) (d)

Fig. 13. CGTS solid skinning (*Duck*). (a) The given cross-sectional T-spline surfaces. (b) The skinned T-spline solid with the mesh generated from the knots. (c) Transparent skinned solid with the given surfaces. (d) Cut-away view of the skinned solid.

Table 3. Statistical data of CGTS solid skinning.

Model	#Given surfaces[a]	#Control points[b]	μ	ν	min_Jac.[c]		max_Jac.[d]		avg_Jac.[e]	
					before[f]	after[g]	before	after	before	after
S shape	7	6519	0.495	0.495	-1.0000	0.6084	1.0000	1.0000	0.8958	0.9623
Moai	6	21345	0.495	0.495	-0.3012	0.0115	1.0000	1.0000	0.9604	0.9643
Tooth	6	10542	0.495	0.495	-0.9280	0.0871	1.0000	1.0000	0.9583	0.9631
Duck	6	9960	0.495	0.495	-1.0000	0.0094	1.0000	1.0000	0.8835	0.9071

[a] Number of the given surfaces.
[b] Number of the control points.
[c] Minimum scaled Jacobian value.
[d] Maximum scaled Jacobian value.
[e] Averaged scaled Jacobian value.
[f] Before the optimization.
[g] After the optimization.

[12] Yang, X, Zheng, J. Approximate T-spline surface skinning. Computer-Aided Design 2012;44(12):1269–1276.
[13] Engleitner, N, Jüttler, B. Lofting with patchwork B-splines. Advanced Methods for Geometric Modeling and Numerical Simulation 2019;:77–98.
[14] Li, Y, Chen, W, Cai, Y, Nasri, A, Zheng, J. Surface skinning using periodic T-spline in semi-NURBS form. Journal of Computational & Applied Mathematics 2015;273(C):116–131.
[15] Dyn, N, Levin, D, Gregory, JA. A 4-point interpolatory subdivision scheme for curve design. Computer Aided Geometric Design 1987;4(4):257–268.
[16] Hughes, TJR, Cottrell, JA, Bazilevs, Y. Isogeometric analysis: CAD, finite elements, NURBS, exact geometry and mesh refinement. Computer Methods in Applied Mechanics & Engineering 2005;194(39):4135–4195.
[17] Zhang, Y, Bazilevs, Y, Goswami, S, Bajaj, CL, Hughes, TJ. Patient-specific vascular NURBS modeling for isogeometric analysis of blood flow. Computer methods in applied mechanics and engineering 2007;196(29):2943–2959.
[18] Martin, T, Cohen, E, Kirby, RM. Volumetric parameterization and trivariate B-spline fitting using harmonic functions. Computer Aided Geometric Design 2009;26(6):648–664.
[19] Aigner, M, Heinrich, C, Jüttler, B, Pilgerstorfer, E, Simeon, B, Vuong, AV. Swept volume parameterization for isogeometric analysis. In: Mathematics of Surfaces XIII. Berlin, Heidelberg: Springer Berlin Heidelberg; 2009, p. 19–44.
[20] Xu, G, Mourrain, B, Duvigneau, R, Galligo, A. Analysis-suitable volume parameterization of multi-block computational domain in isogeometric applications. Computer-Aided Design 2013;45(2):395–404.
[21] Wang, X, Qian, X. An optimization approach for constructing trivariate B-spline solids. Computer-Aided Design 2014;46(1):179–191.
[22] Lin, H, Jin, S, Hu, Q, Liu, Z. Constructing B-spline solids from tetrahedral meshes for isogeometric analysis. Computer Aided Geometric Design 2015;35-36:109–120.
[23] Lin, H, Huang, H, Hu, C. Constructing trivariate B-splines with positive Jacobian by pillow operation and geometric iterative fitting. arXiv preprint arxiv:181112597v1 2018;.
[24] Lin, H, Huang, H, Hu, C. Trivariate B-spline solid construction by pillow operation and geometric iterative fitting. SCIENCE CHINA (Information Sciences) 2018;61:232–234.
[25] Escobar, J, Cascón, J, Rodríguez, E, Montenegro, R. A new approach to solid modeling with trivariate T-splines based on mesh optimization. Computer Methods in Applied Mechanics and Engineering 2011;200(45):3210 – 3222.
[26] Zhang, Y, Wang, W, Hughes, TJ. Solid T-spline construction from boundary representations for genus-zero geometry. Computer Methods in Applied Mechanics & Engineering 2012;249-252(s 249C252):185–197.
[27] Wang, W, Zhang, Y, Liu, L, Hughes, TJR. Trivariate solid T-spline construction from boundary triangulations with arbitrary genus topology. Computer-Aided Design 2013;45(2):351–360.
[28] Lin, H, Wang, G, Dong, C. Constructing iterative non-uniform B-spline curve and surface to fit data points. Science in China 2004;47(3):315–331.
[29] Lin, H, Bao, H, Wang, G. Totally positive bases and progressive iteration approximation. Computers & Mathematics with Applications 2005;50(3):575–586.
[30] Shi, LM. An iterative algorithm of NURBS interpolation and approximation. Journal of Mathematical Research & Exposition 2006;26(4).
[31] Lin, H. Local progressive-iterative approximation format for blending curves and patches. Computer Aided Geometric Design 2010;27(4):322–339.
[32] Chen, Z, Luo, X, Le, T, Ye, B, Chen, J. Progressive interpolation based on Catmull-Clark subdivision surfaces. Computer Graphics Forum 2010;27(7):1823–1827.
[33] Lin, H, Zhang, Z. An extended iterative format for the progressive-iteration approximation. Computers & Graphics 2011;35(5):967–975.
[34] Sederberg, TW, Cardon, DL, Finnigan, GT, North, NS, Zheng, J, Lyche, T. T-spline simplification and local refinement. Acm Transactions on Graphics 2004;23(3):276–283.
[35] Farin, G. Curves and surfaces for computer aided geometric design: a practical guide. 1993.
[36] Knupp, PM. A method for hexahedral mesh shape optimization. International Journal for Numerical Methods in Engineering 2003;58(2):319–332.